Dissipation-induced hard-core boson gas in an optical lattice

2009 New J. Phys. 11 013053

(http://iopscience.iop.org/1367-2630/11/1/013053)

New Journal of Physics
The open-access journal for physics

Dissipation-induced hard-core boson gas in an optical lattice

J J García-Ripoll[1,2,3,4], S Dürr[2], N Syassen[2], D M Bauer[2], M Lettner[2], G Rempe[2] and J I Cirac[2]

[1] Facultad de Ciencias Físicas, Universidad Complutense de Madrid, Ciudad Universitaria, E-28040, Madrid, Spain
[2] Max-Planck-Institut für Quantenoptik, Hans-Kopfermann-Strasse 1, 85748 Garching, Germany
E-mail: juanjose.garciaripoll@gmail.com

New Journal of Physics **11** (2009) 013053 (19pp)
Received 22 September 2008
Published 30 January 2009
Online at http://www.njp.org/
doi:10.1088/1367-2630/11/1/013053

Abstract. We present a theoretical investigation of a lattice Tonks–Girardeau gas that is created by inelastic, instead of elastic interactions. An analytical calculation shows that in the limit of strong two-body losses, the dynamics of the system is effectively that of a hard-core boson gas. We also derive an analytic expression for the effective loss rate. We find good agreement between these analytical results and results from a rigorous numerical calculation. The hard-core character of the particles is visible both in a reduced effective loss rate and in the momentum distribution of the gas.

[3] Present address: Instituto de Física Fundamental, CSIC, c/Serrano 113b, Madrid, Spain.
[4] Author to whom any correspondence should be addressed.

Contents

1. Introduction

In the field of ultracold atoms, 'Tonks–Girardeau gas' is a term used to describe a one-dimensional (1D) gas of identical bosons where a repulsive interaction dominates all other energy scales. The term Tonks–Girardeau stems from the studies of gases made of impenetrable particles by Tonks [1] and by Girardeau [2], who respectively analyzed the classical and quantum versions of these models. In particular, the term stresses the fact that the wavefunction of 1D hard-core bosons can be exactly mapped to that of an identical fermionic model [2]. The mapping by Girardeau, similar in spirit to the Jordan–Wigner transform of a lattice gas [3], reveals the complete 'fermionization' of the bosonic system, which has the same dynamics and excitation spectrum as its fermionic counterpart. We can thus say that in 1D, a strong repulsion is equivalent to a Pauli exclusion principle. However, we do not need infinite strength interactions to observe this effective fermionization. The exact solution of the 1D bosons with contact interactions by Lieb and Liniger [4] shows that it suffices to increase the ratio of interaction to kinetic energy, either with a stronger repulsion between bosons or by lowering the density. Both approaches, that is diminishing the kinetic energy with an optical lattice and lowering the density by confining the particles in very long tubes, have made it possible to observe a Tonks–Girardeau gas of ultracold atoms [5]–[7].

In a recent experiment [8], we showed that strong dissipation in the form of two-body losses can also simulate a Pauli exclusion principle, fermionizing a system and transforming it

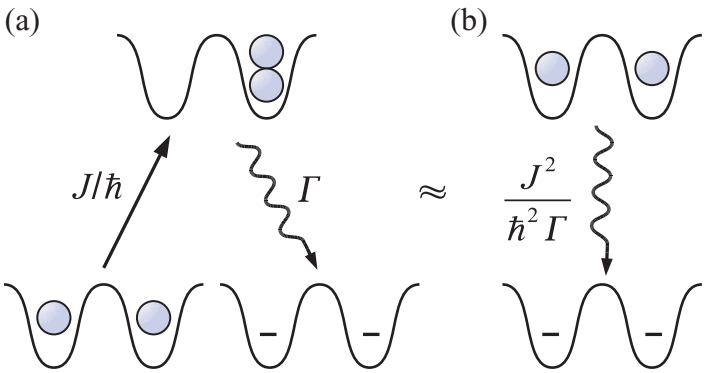

Figure 1. Two molecules sit on neighboring lattice sites. The molecules can tunnel with a hopping amplitude $J/\hbar$ which is much weaker than the decay rate of the resulting doubly occupied site into the vacuum. The effective model is that of impenetrable particles decaying with a much weaker $\mathcal{O}(J^2/\hbar^2\Gamma)$ decay rate.

into a dissipative but long-lived strongly correlated gas. This equivalence was demonstrated for molecules of ^{87}Rb loaded in an optical lattice. For deep enough lattices, these particles exhibit strong two-body decay rates which, in appropriate units, exceed the average kinetic energy of the particles. The particles then avoid coming close together and behave like impenetrable bosons. This happens both in the continuum case of 1D tubes and when the tubes are modulated by a deep optical lattice—two situations which resemble the experiments with elastically interacting bosonic atoms in [6, 7] and [5], respectively.

At least in the lattice case, the equivalence between strong dissipation and a Pauli exclusion principle can be understood in terms of the Zeno effect. Following the discussion in [8], figure 1 depicts a stable configuration with two molecules on neighboring sites. This configuration is connected via hopping to states with double occupancy. These states decay at a rate Γ, which is much larger than the hopping amplitude $J/\hbar$ of the particles. Treating this as a typical three-level system from quantum optics, one concludes that particles stay on their original sites with only a minor loss rate of $\mathcal{O}(J^2/\hbar^2\Gamma)$.

In this work, we present a rigorous theoretical analysis of this system. The outline is as follows. We begin in section 2 by introducing a master equation that models two-body losses for a single species of bosonic particles—for instance the molecules in [8]. We will particularize the model to the case in which particles are confined by an optical lattice and explain how dissipation becomes the dominant term. In section 3, we will show that in the limit of strong losses the master equation can be replaced by an effective model in which the rapid two-body decay has been eliminated. The dominant terms of the effective model are identical to the Hamiltonian of an elastic Tonks–Girardeau gas. The residual effect of losses is a slow perturbation that can be obtained analytically. In section 4, we compare both results to exact numerical simulations of the full master equation. We use matrix product density operators (MPDO) [9] to verify that both the density and momentum distributions of the particles closely resemble those of a Tonks–Girardeau gas. A second signature of the hard-core boson dynamics is a slowdown of the inelastic losses, for which we find good agreement between numerical and analytical estimates. In the last part of our work, we provide further details about the methods and derivation used to obtain the effective Tonks–Girardeau gas models and the slowdown of losses. Finally, we summarize this paper in section 6.

2. Formalism

2.1. Master equation

We model the dynamics of the particles using a Markovian master equation

$$\hbar\frac{\mathrm{d}\rho}{\mathrm{d}t} = -\mathrm{i}[H,\rho]+\mathcal{D}\rho, \tag{1}$$

where H is the Hamiltonian describing the unitary part of the evolution and $\mathcal{D}$ is a dissipator associated with the losses due to inelastic collisions. In the absence of a lattice potential [10]

$$H = \int \mathrm{d}^3x\,\Psi^\dagger H_\mathrm{s}\Psi + \frac{\mathrm{Re}(g_\mathrm{3D})}{2}\int \mathrm{d}^3x\,\Psi^{\dagger 2}\Psi^2, \tag{2}$$

$$\mathcal{D}\rho = -\frac{\mathrm{Im}(g_\mathrm{3D})}{2}\int \mathrm{d}^3x\left(2\Psi^2\rho\Psi^{\dagger 2} - \Psi^{\dagger 2}\Psi^2\rho - \rho\Psi^{\dagger 2}\Psi^2\right), \tag{3}$$

where $H_\mathrm{s}(\mathbf{x}) = -\hbar^2\nabla^2/2m + V_\mathrm{trap}(\mathbf{x})$ is the single-particle Hamiltonian and $\Psi(\mathbf{x})$ is the bosonic field operator. The strength of the interparticle interactions is $g_\mathrm{3D} = 4\pi\hbar^2 a/m$, where m is the mass of a particle and a is the scattering length. $\mathrm{Re}(a)$ describes elastic collisions, whereas $\mathrm{Im}(a) \leqslant 0$ describes inelastic collisions that lead to losses.

To assert the consistency of this model, let us estimate the decay rate of the particles. When taking expectation values over the density operator, $n(x) = \Psi^\dagger(\mathbf{x})\Psi(\mathbf{x})$, the previous master equation becomes

$$\frac{\mathrm{d}}{\mathrm{d}t}\langle\Psi^\dagger(\mathbf{x})\Psi(\mathbf{x})\rangle = \frac{2}{\hbar}\,\mathrm{Im}(g_\mathrm{3D})\langle\Psi^{\dagger 2}(\mathbf{x})\Psi^2(\mathbf{x})\rangle. \tag{4}$$

For a condensate of molecules, this gets the expected form

$$\frac{\mathrm{d}}{\mathrm{d}t}\bar{n}(\mathbf{x}) \simeq -K_\mathrm{3D}\bar{n}(\mathbf{x})^2, \tag{5}$$

where $\bar{n}(\mathbf{x})$ is the density of bosons at a given point and the decay rate is proportional to the square of the density and to $K_\mathrm{3D} = -2\,\mathrm{Im}(g_\mathrm{3D})/\hbar$.

Note in passing that the dissipation that we are considering here is loss of particles. It is thus both formally and conceptually different from the Caldeira–Leggett type of models that has been introduced in the literature [11] and generalized to many-body systems (see [12] and references therein), and where dissipation appears in the form of a friction caused by one or more thermal baths.

2.2. Optical lattice

As explained in the introduction, in this paper we want to model the experiment with molecules in a deep optical lattice [8]. For low temperatures and tight confinements, we can expect that the particles will accommodate to the motional ground state of each lattice site. Note that if this is true for individual atoms, it is even more so for molecules, because having twice the mass and twice the polarizability, they are better trapped by the same optical potential. Under these conditions, it was shown in [13] that it is convenient to expand the bosonic field operator $\Psi^\dagger$ using Fock operators, $a_k^\dagger$, that create particles on the kth lattice site:

$$\Psi^\dagger(\mathbf{x}) = \sum_k a_k^\dagger w(\mathbf{x}-\mathbf{x}_k). \tag{6}$$

The $w(\mathbf{x})$ are Wannier wavefunctions associated with the states localized on each site. In particular, for the arrays of 1D lattices used in [8], we can separate the wavefunction of these bosonic modes into a product of three wavepackets, $w(\mathbf{x}) = w_{\parallel}(x)w_{\perp}(y)w_{\perp}(z)$, a less confined longitudinal one, $w_{\parallel}$, and two transverse ones, $w_{\perp}$, which are very tight due to the perfect decoupling between adjacent tubes.

The advantage of the Wannier functions is that we can now perform a tight-binding approximation: anywhere outside the single-particle terms in the Hamiltonian, the overlap of different Wannier functions is neglected. This procedure transforms the unitary part of the master equation into a Bose–Hubbard model [13], and discretizes the dissipative terms as well

$$\begin{aligned} H &= -J\sum_{\langle k,l\rangle} a_k^\dagger a_l + \frac{U_\mathrm{r}}{2}\sum_k a_k^{\dagger 2} a_k^2, \\ \mathcal{D}\rho &= \frac{\hbar\Gamma}{4}\sum_k (2a_k^2\rho a_k^{\dagger 2} - a_k^{\dagger 2}a_k^2\rho - \rho a_k^{\dagger 2}a_k^2). \end{aligned} \tag{7}$$

Regarding the notation, the sum $\langle k, l\rangle$ extends over nearest neighbors along the same tube, $|k-l| = 1$. The tunneling amplitude between neighboring lattice sites is denoted by J. Finally, the on-site interaction matrix element contains both real and imaginary parts:

$$U = g_{3\mathrm{D}}\int \mathrm{d}x\,|w_{\parallel}(x)|^4\left[\int \mathrm{d}y\,|w_{\perp}(y)|^4\right]^2 = U_\mathrm{r} + \mathrm{i}U_\mathrm{i} = U_\mathrm{r} - \mathrm{i}\frac{\hbar\Gamma}{2}, \tag{8}$$

which contribute to the unitary and the dissipative parts of the master equation, respectively.

The imaginary part of the interaction constant governs the decay of the number of particles per site, $n_k = a_k^\dagger a_k$

$$\frac{\mathrm{d}}{\mathrm{d}t}\langle n_k\rangle = -\Gamma\langle n_k(n_k-1)\rangle. \tag{9}$$

In the cases that we will study this rate will be larger than the speed at which particles tunnel to neighboring sites, $\Gamma \gg J/\hbar$. To facilitate the calculations, we will group the terms in the master equation according to their strength. We introduce a superoperator $\mathcal{V}$ that contains the tunneling part ($H_J \propto J$) and a superoperator $\mathcal{L}_\mathrm{int}$ that describes the elastic ($H_\mathrm{el} \propto U_\mathrm{r}$) and inelastic interactions ($\mathcal{D} \propto \Gamma$):

$$\frac{\mathrm{d}}{\mathrm{d}t}\rho = (\mathcal{V} + \mathcal{L}_\mathrm{int})\,\rho, \tag{10a}$$

$$\mathcal{V}\rho = -\frac{\mathrm{i}}{\hbar}[H_J, \rho], \tag{10b}$$

$$\mathcal{L}_\mathrm{int}\rho = -\frac{\mathrm{i}}{\hbar}[H_\mathrm{el}, \rho] + \frac{1}{\hbar}\mathcal{D}\rho. \tag{10c}$$

The term 'superoperator' refers to the fact that $\mathcal{D}$, $\mathcal{V}$ and $\mathcal{L}_\mathrm{int}$ are linear operators acting on density matrices, not on pure states. Finally, it is important to realize that $\mathcal{V}$ is of order J, whereas $\mathcal{L}_\mathrm{int}$ is of order $|U| \gg |J|$, and dominates the evolution. The following sections exploit this difference of scales to create new and simpler effective models that describe the dynamics of the molecules.

3. Effective models

3.1. Second-order effective theory

Our goal is to develop an effective master equation that is equivalent to (10*a*) in the limit of strong dissipation, $\hbar\Gamma \gg J$, in which $\mathcal{L}_{\rm int}$ dominates. We will sketch the main ideas and refer the reader to section 5 for more details. The process begins by identifying the eigenvalues, λ_i, and eigenspaces of the dominant term, $\mathcal{L}_{\rm int} = \sum_i \lambda_i \mathcal{P}_i$. We then decompose the density matrix into a sum of contributions from these eigenspaces

$$\rho(t) = \sum_i \rho_i(t) = \sum_i \mathcal{P}_i \rho(t). \tag{11}$$

Finally, we will determine some approximate evolution equations for the different ρ_i in the presence of a nonzero hopping term, $\mathcal{V}$.

We only need to study three eigenspaces, corresponding to the dissipation-less states, $\lambda_0 = 0$, and to the states most immediately connected to them by the hopping. The most relevant term of our density matrix, $\rho_0 \sim \mathcal{O}(1)$, is given by states with zero or one particle per site. These states do not decay in the absence of hopping, since they have at most one particle per site. Formally, we write

$$\rho_0 = Q_0 \rho Q_0 \tag{12}$$

with a projector expressed in the Fock basis of occupation numbers

$$Q_0 = (|0\rangle\langle 0| + |1\rangle\langle 1|)^{\otimes L} = q_0^{\otimes L}, \tag{13}$$

where L is the number of sites in the lattice. The next states that we need to consider have a pair of particles on some site. As we will see later, we have two sets of states depending on whether the double occupation is on the left or on the right side of the matrix coherences

$$\begin{aligned} \mathcal{P}_{1a}\rho &= Q_1\, \rho\, Q_0, \\ \mathcal{P}_{1b}\rho &= Q_0\, \rho\, Q_1, \end{aligned} \tag{14}$$

where we have introduced

$$Q_1 = \sum_{k=0}^{L} q_0^{\otimes k-1} \otimes |2\rangle\langle 2| \otimes q_0^{L-k}. \tag{15}$$

In the absence of hopping these states decay with eigenvalues $\lambda_{1a} = -\Gamma/2 - \mathrm{i}U_{\rm r}/\hbar = -\mathrm{i}U/\hbar$ and $\lambda_{1b} = -\Gamma/2 + \mathrm{i}U_{\rm r}/\hbar = \mathrm{i}U^*/\hbar$, respectively.

By neglecting higher order contributions to the density matrix, it is possible to integrate formally the projected master equation and obtain an effective model for the dominant term, $\rho_0(t)$. After some manipulations one arrives at the following model (section 5.3):

$$\frac{\mathrm{d}\rho_0}{\mathrm{d}t} = (\mathcal{L}_1 + \mathcal{L}_2)\rho_0, \tag{16a}$$

$$\mathcal{L}_1 = \mathcal{P}_0 \mathcal{V} \mathcal{P}_0, \tag{16b}$$

$$\mathcal{L}_2 = \sum_{c\in\{1a,1b\}} \frac{-1}{\lambda_c} \mathcal{P}_0 \mathcal{V} \mathcal{P}_c \mathcal{V} \mathcal{P}_0. \tag{16c}$$

We will now write down explicitly and discuss the meaning and implications of these different terms.

3.2. Tonks–Girardeau gas

The most important term in our effective model (16*a*) is given by the Liouville operator $\mathcal{L}_1 = \mathcal{P}_0 \mathcal{V} \mathcal{P}_0$. As shown in section 5.4 this superoperator is equivalent to a Hamiltonian of hard-core bosons, also known as a Tonks–Girardeau gas. Therefore, to lowest order

$$\frac{\mathrm{d}}{\mathrm{d}t}\rho_0 = -\frac{\mathrm{i}}{\hbar}\left[-J\sum_{\langle k,l\rangle} c_k^\dagger c_l,\, \rho_0\right] + \mathcal{O}\left(J^2/|U|\right), \tag{17}$$

with bosonic operators $c_k^\dagger$ and c_k that carry the hard-core constraint

$$c_k|0\rangle_k\langle 1|_k, \quad c_k^\dagger = |1\rangle_k\langle 0|_k. \tag{18}$$

This is the main result of our paper. Namely, that a strong dissipation such as the two-body losses from our system can lead to coherent evolution. As was mentioned in the introduction, the same result can be obtained in an alternative way. By establishing an analogy between losses and a continuous measurement, it is intuitively clear that the strong dissipation causes a Zeno effect which suppresses the process of two particles coming together and being lost. In this regime, the dynamics of the molecules must be given by a Hubbard model where doubly occupied states have been projected out.

In practice, the hard-core boson model implies a very simple dynamics that can be tested numerically, as we do in section 4. However, verifying the same thing with real particles in an optical lattice represents a challenging experiment. Nevertheless, one can easily check two phenomena: firstly, that in the regime of strong decay, $\hbar\Gamma \gg J$, no significant losses take place on a timescale of order $1/\Gamma$ and secondly, that the effective loss rate can be estimated using the second part of our effective model (16*a*)–(16*c*). This is the goal of the following sections.

3.3. Second-order corrections

With a lengthy calculation we can rewrite the second-order terms in equation (16*a*) as an effective Liouvillian $\mathcal{L}_2$ with both a Hamiltonian and dissipation:

$$\mathcal{L}_2\rho_0 = -\frac{\mathrm{i}}{\hbar}[H_2,\, \rho_0] + \frac{1}{\hbar}\mathcal{D}_2\rho_0. \tag{19}$$

It is convenient to introduce an operator that destroys a pair of particles in neighboring sites

$$C_k = c_k(c_{k+1} + c_{k-1}). \tag{20}$$

With these pairs the Hamiltonian part can be written as

$$H_2 = -J_2\sum_k C_k^\dagger C_k, \tag{21}$$

with an effective strength $(1/\lambda_{1a} = \hbar\mathrm{i}/U)$

$$J_2 = \frac{2J^2}{\hbar}\mathrm{Im}\left(\frac{1}{\lambda_{1a}}\right) = \frac{2J^2}{|U|^2}U_\mathrm{r}. \tag{22}$$

Note that this Hamiltonian contains both effective nearest-neighbor interactions and a three-site hopping of the form $c_{k+1}^\dagger n_k c_{k-1}$. Both terms are typical of the Bose–Hubbard model in the limit of strong repulsive interaction $U_\mathrm{r} \gg |J|$ [14]. Moreover, these Hamiltonian corrections disappear when the lossy particles do not interact elastically on-site, $U_\mathrm{r} = 0$.

The dissipative term is equally simple,

$$\mathcal{D}_2\rho_0 = \hbar\Gamma_2 \sum_k \left(2C_k\rho_0 C_k^\dagger - C_k^\dagger C_k\rho_0 - \rho_0 C_k^\dagger C_k\right), \tag{23}$$

and has a loss coefficient

$$\Gamma_2 = -\frac{2J^2}{\hbar^2}\mathrm{Re}\left(\frac{1}{\lambda_{1a}}\right) = -\frac{2J^2}{\hbar|U|^2}U_\mathrm{i}. \tag{24}$$

In the limit of weak elastic interaction between molecules we may write

$$\Gamma_2 = -\frac{2J^2}{\hbar U_\mathrm{i}}\left(1+\frac{U_\mathrm{r}^2}{U_\mathrm{i}^2}\right)^{-1} = \frac{4J^2}{\hbar^2\Gamma}\left(1+\frac{4U_\mathrm{r}^2}{\hbar^2\Gamma^2}\right)^{-1}, \tag{25}$$

which shows that the decay rate is indeed $\mathcal{O}(J^2/\hbar^2\Gamma)$ as anticipated.

3.4. Effective losses

Let us write the evolution of the total number of particles, $\hat{N}$, under the effective master equation (16*a*)

$$\frac{\mathrm{d}}{\mathrm{d}t}\langle\hat{N}\rangle = -\sum_k \Gamma_2\langle[C_k^\dagger C_k, \hat{N}]\rangle = -4\Gamma_2\sum_k\langle C_k^\dagger C_k\rangle. \tag{26}$$

This expression in general cannot be simplified any further, at least not without some assumption about the state with which we compute the expectation value.

The experiments described in [8] start from a state with exactly one molecule at each site and evolve only until approximately half of the particles are lost. Here further approximations are possible: firstly we treat the system as homogeneous and secondly we assume that the populations of different sites are uncorrelated[5]. We thus obtain

$$\langle C_k^\dagger C_k\rangle = \sum_{l,l'\in\{k-1,k+1\}}\langle c_k^\dagger c_l^\dagger c_k c_{l'}\rangle \simeq z\bar{n}^2, \tag{27}$$

where $\bar{n}$ is the density and $z=2$ is the coordination number of our lattice. This approximation leads to a rate equation which is typical in two-body processes

$$\frac{\mathrm{d}}{\mathrm{d}t}\bar{n} \simeq -4z\Gamma_2\bar{n}^2 \equiv -\kappa\bar{n}^2. \tag{28}$$

A similar equation was derived previously in [8] using a more limited theory than our effective master equation (16*a*).

4. Numerical results

In order to study the quality of the approximations used in the effective model, we have performed numerical simulations of the full master equation (10*a*) using MPDO [9]. This is a method that approximates the density matrix $\rho(t)$ using a matrix product state structure. As described in [9], this variational ansatz is well suited to simulating evolution of a state under a Liouvillian like $\mathcal{V}+\mathcal{L}_\mathrm{int}$, which can be decomposed into a sum of local or nearest-neighbor

[5] Note that this does not imply that the particles themselves are uncorrelated.

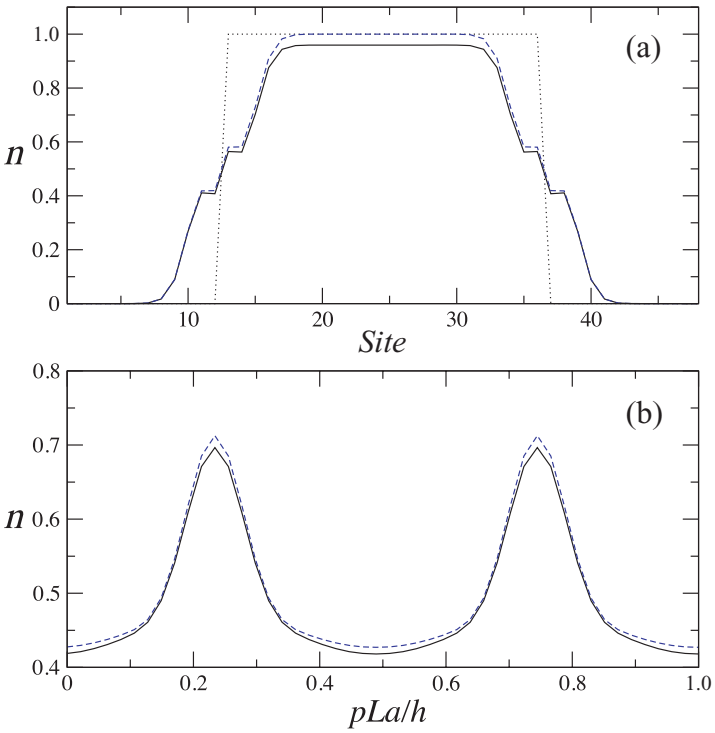

Figure 2. Comparison between the dissipative system (solid lines) and the lossless Tonks–Girardeau gas (dashed lines). $N = 24$ central sites of the lattice initially contain exactly one particle per site (dotted line in (a)). The system is evolved with $\hbar\Gamma/J = 4000$ for a time $t = 2\hbar/J$. The evolution is simulated either with the full master equation (10*a*) or with the lossless Tonks–Girardeau model equation (17). Part (a) shows the position distribution versus site index, part (b) the momentum distribution versus quasi-momentum p (a is the lattice spacing and L the lattice length), both after the time evolution. The difference between the distributions is marginal, except for an overall reduction of particle number.

terms. In our simulations, we have worked with up to 48 sites and open boundary conditions, setting $U_r = 0$ so that the different effects cannot be attributed to a repulsive interaction. We have experimented with different cutoffs, from two to four particles per site, verifying that they give similar results.

4.1. Comparison with the lossless Tonks–Girardeau gas

Figure 2 shows numerical results for $\hbar\Gamma/J = 4000$. The system was initially prepared such that the $N = 24$ central sites of the lattice contain one particle per lattice site, while all other lattice sites are empty, similar to the state experimentally prepared in [15]. We then let the system evolve for a time $t = 2\hbar/J$ and measure both the density and the momentum distributions, which are plotted in figures 2(a) and (b), respectively. The solid lines were obtained with the full master equation (10*a*) and differ only slightly from the dashed lines obtained with the lossless Tonks–Girardeau model of equation (17). The observed difference in the distributions is largely due to the reduced particle number.

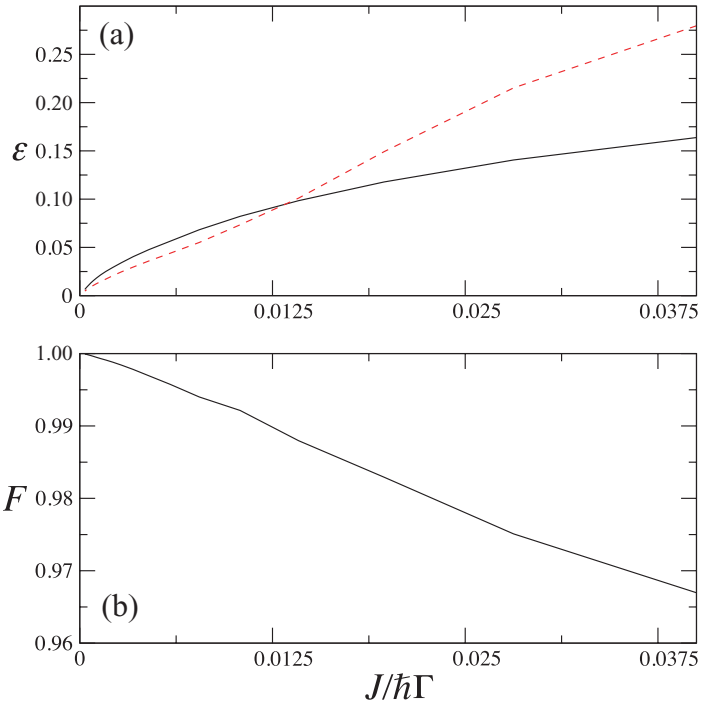

Figure 3. (a) Difference between the distributions of the dissipative system and the lossless Tonks–Girardeau gas. Calculations as in figure 2 for a variety of values $J/\hbar\Gamma$. Each yields a different distribution for the dissipative system and the lossless Tonks–Girardeau gas. The value ϵ defined in equation (29) quantifies this difference for the position distribution (solid line) and the momentum distribution (dashed line). (b) Fraction of the density matrix in the hard-core bosons subspace, with F defined in equation (30). $1-F$ is typically smaller than ϵ.

In order to quantify the difference in the distributions of particles, we define

$$\epsilon = \sum_{x=1}^{L} \left| \frac{n_x}{N(t)} - \frac{n_x^{\text{Tonks}}}{N(0)} \right|, \tag{29}$$

where $N(t)$ is the total number of particles at a given time, n_x is the number of particles for the site x and n_x^{Tonks} is the same for the lossless Tonks–Girardeau gas. A similar measure can be defined in momentum space. Figure 3(a) shows these quantities. For $J/\Gamma \to 0$ the distributions converge to those of a lossless Tonks–Girardeau gas, as expected from the effective model.

Another relevant quantity is the fraction of the state that lives in the subspace with the hard-core constraint of one or zero particles per site

$$F = \text{Tr}(Q_0\rho). \tag{30}$$

This quantity is shown in figure 3(b). Comparison with figure 3(a) shows that $1-F$ tends to be much smaller than ϵ. Our interpretation is that the loss of particles causes the system to evolve into an incoherent mixture of states with different total particle number. While each of the contributions in this mixture satisfies pretty well the hard-core constraint and thus F is small, they all have different density and momentum distribution, leading to large values in ϵ.

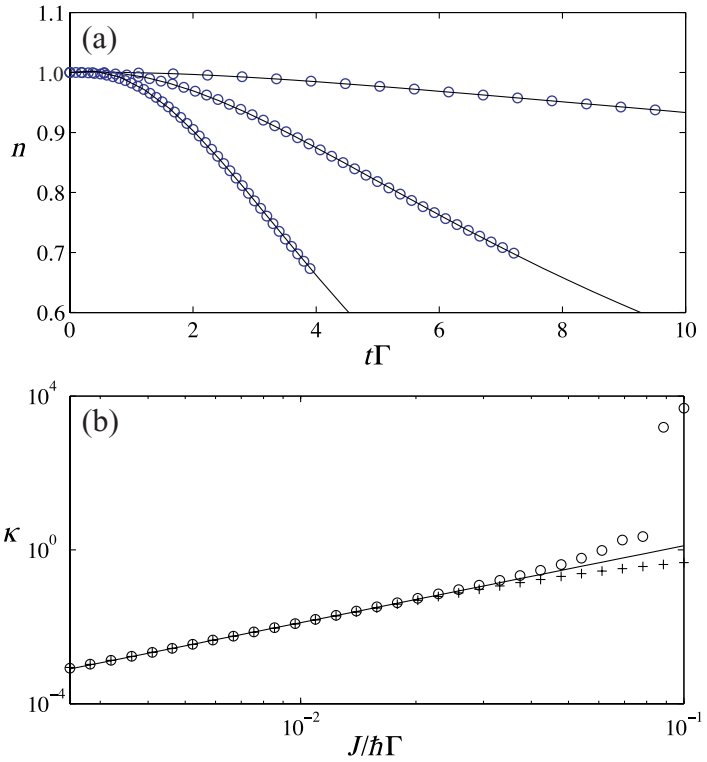

Figure 4. We study the density as a function of time, for a simulation of equation (1) using $L = 40$ sites, each one initially filled with exactly one particle. (a) Evolution of the density as a function of the adimensionalized time $t\Gamma$, for three values of the losses $J/\hbar\Gamma = 0.0179$, 0.0541 and 0.1 (from top to bottom). We present data from both the numerical simulation and for a fit with equation (34), using circles and lines, respectively. (b) Best-fit values of the effective decay rate κ versus the value of $J/\hbar\Gamma$ at which the simulation took place. The solid line represents the theoretical prediction equation (28). The crosses and the circles correspond to fits using the formulae in equations (32) and (34), respectively.

4.2. Effective loss rate

Our analytic model suggests that the loss rate for the particle number in a homogeneous system can be approximated by a two-body decay equation (28). The solution of this equation is given by

$$\bar{n}(t) = \frac{\bar{n}(0)}{1 + \bar{n}(0)\kappa t}, \tag{31}$$

This result applies to the case in which different sites are not very correlated and the losses Γ dominate over the hopping, J.

In order to test this prediction, we have performed MPDO simulation of equation (10*a*) using a uniformly filled lattice with $L = 40$ sites and $N = 40$ particles. We studied the evolution for a wide range of values of $J/\hbar\Gamma$, with some examples shown in figure 4(a). After an initial transient that vanishes on a timescale $\approx 1/\Gamma$, the two-body decay equation (28) fits the data fairly well. However, while for $J/\hbar\Gamma \ll 1$ the effect of the transient is negligible, for larger

$J/\hbar\Gamma$ there are better ways to fit the resulting curves. One possibility, used in [8] to fit the numerical data, is to include a free parameter t_0 describing an offset along the time axis

$$\bar{n}(t) = \frac{\bar{n}(0)}{1+\bar{n}(0)\kappa(t-t_0)}. \tag{32}$$

However, we found that a more accurate model is a modified decay equation with an exponentially modulated decay coefficient

$$\frac{\mathrm{d}}{\mathrm{d}t}\bar{n} = -\kappa(1-\mathrm{e}^{-\lambda t})\bar{n}^2. \tag{33}$$

Here the exponential term with $\lambda \sim \Gamma$ represents an heuristic approximation to the transients that we have neglected in developing the effective model (see section 5.3). The solution of this differential equation still has two fit parameters

$$\bar{n}(t) = \frac{\bar{n}(0)}{1+\bar{n}(0)\kappa\{t+[\exp(-\lambda t)-1]/\lambda\}}. \tag{34}$$

Figure 4(b) shows the loss rate coefficient κ from these two fits and figure 4(a) shows the quality of the fits for small values of the hopping. For larger values, though, the fitting becomes numerically unstable and it is better to use the single-parameter fit (32).

What we do not show in the previous plots is that the long-term behavior of the system no longer follows the simple two-body decay laws from equations (32) and (34). The reason is that at low densities there are enough correlations that we can no longer use the simple models from section 3.3. In this regime of small densities, a coarse grained description becomes approximately equivalent to the Lieb–Liniger model [14] but with inelastic interactions. As we have shown elsewhere [8], the decay at long times is then expected to follow the law $\mathrm{d}\bar{n}/\mathrm{d}t \propto \bar{n}^4$.

5. Detailed calculations

The goal of this work is to find an effective model for the particles in the lattice, which works in the limit of fast dissipation, $J \ll \hbar\Gamma$. Our main tool to understand this limit is a generalization of Kato perturbation theory [16], also known as adiabatic elimination, to the superoperators $\mathcal{V}$ and $\mathcal{L}_{\mathrm{int}}$. Section 5.1 explains how our calculations relate to this broader scope. Readers less interested in this aspect may skip to section 5.2 where the actual derivation begins.

5.1. General ideas

Both $\mathcal{V}$ and $\mathcal{L}_{\mathrm{int}}$ are linear operators that act on an appropriate space of matrices. Even though within this space the superoperators are not Hermitian, the dominant term $\mathcal{L}_{\mathrm{int}}$ has infinitely many eigenstates. They form a discrete spectrum of well separated points that begin at $\lambda_0 = 0$ and span through the left half of the complex plane (figure 5(b)). Each of these points represents a family of matrices that, in the absence of a hopping term, decay at a rate given by the real part of the eigenvalue, $\mathrm{Re}(\lambda_i) \leqslant 0$. In the limit of strong dissipation, the hopping $\mathcal{V}$ will couple these eigenspaces very weakly, with an amplitude $J/\hbar$ much smaller than the typical eigenvalue separation, Γ.

Precisely, in this limit of weak hopping, we will be able to write analytic expansions of the eigenstates, eigenvalues and evolution equations for the perturbed superoperator $(\mathcal{V}+\mathcal{L}_{\mathrm{int}})$. The

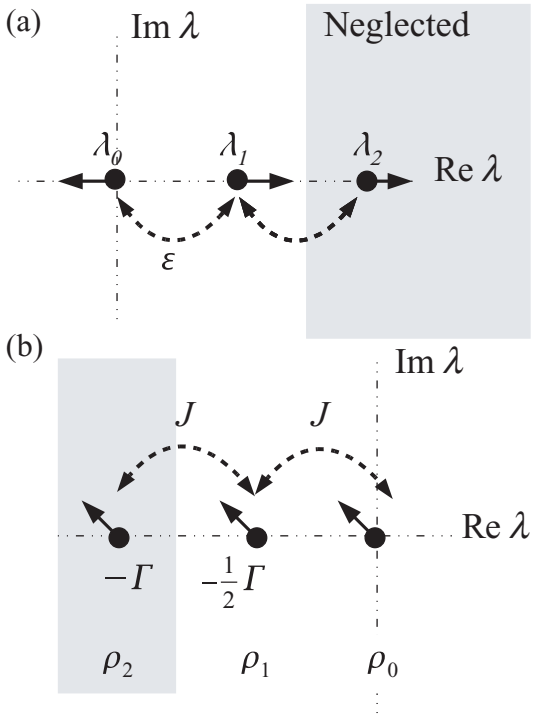

Figure 5. (a) In ordinary perturbation theory of Hermitian operators we find eigenspaces with eigenvalues which are well separated along the real axis. A weak Hermitian coupling, smaller than the energy separation between spaces $\varepsilon \ll |\lambda_i - \lambda_j|$, only causes small shifts in these energy levels. (b) Our Liouville operator $\mathcal{L}_{\rm int}$ is not Hermitian but has well separated eigenvalues in the space of density matrices (we have set $U_{\rm r} = 0$ for simplicity). The real part of these eigenvalues now represents the decay rate of such matrices. The hopping of particles J acts as a weak perturbation $J \ll \hbar\Gamma$ that slightly changes both the real and the imaginary parts of the original eigenvalues. In particular, the states with one particle per site, ρ_0, now acquire contributions of $\mathcal{O}(J/\Gamma)^1$ and $\mathcal{O}(J/\Gamma)^{2,3,\ldots}$ by coupling directly, ρ_1, or indirectly, $\rho_{2,3,\ldots}$, to faster decaying subspaces. Both in (a) and (b), for second-order approximations of the unperturbed eigenspaces, λ_0, we may neglect all spaces with an indirect coupling.

idea is to use Kato's resolvent method [16] with an expansion of the Liouvillian

$$\mathcal{L}_{\rm int} = \sum_i \lambda_i \mathcal{P}_i, \tag{35}$$

that uses a complete set of pseudo-projector operators

$$\mathcal{P}_i \mathcal{P}_j = \delta_{ij} \mathcal{P}_i, \quad \sum_i \mathcal{P}_i = 1. \tag{36}$$

These operators, built from the right and left eigenvectors of $\mathcal{L}_{\rm int}$, are non-Hermitian but this fact poses no difficulties in generalizing the usual perturbation theory.

In particular, the space of density matrices that had zero decay rate for $J = 0$ will transform into the perturbed eigenstates and eigenvalues

$$(\mathcal{V} + \mathcal{L}_{\rm int})\tilde{\rho}_0(J) = \tilde{\lambda}_0(J)\tilde{\rho}_0(J). \tag{37}$$

The decay rate will no longer be zero but remain small

$$\tilde{\lambda}_0(J) = J \sum_{n>1} c_n \left(\frac{J}{\hbar\Gamma}\right)^n \sim \mathcal{O}(J^2/\hbar\Gamma), \tag{38}$$

and these states will acquire a small admixture of the matrices belonging to the unperturbed eigenspaces that had larger decay rates

$$\tilde{\rho}_0(J) = \rho_0 + \sum_{n>1} \left(\frac{J}{\hbar\Gamma}\right)^n \rho_n. \tag{39}$$

Notice the weight of the different contributions ρ_n depends on how many applications of $\mathcal{V}$ we have to perform to connect ρ_0 to these other eigenspaces. Furthermore, we understand that it is the coupling of ρ_0 to the decaying states through $\mathcal{V}$ that makes the initially stable space lose particles. A similar reasoning can be applied to the rapidly decaying eigenspaces, $\tilde{\rho}_{1,2,\ldots}(J)$, which will be modified by the coupling $\mathcal{V}$. However in this case the decay rates will remain of order Γ with small corrections from the hopping of particles.

We therefore conclude that if we prepare our particles in any initial state, after a short transient $t \sim 1/\Gamma$, most of the state will be captured by the eigenspace with the lowest decay rate (38). Following the structure given in equation (39) we will decompose our evolved state in a series of contributions from the unperturbed eigenspaces

$$\rho(t) = \rho_0(t) + \rho_1(t) + \rho_2(t) + \ldots, \tag{40}$$

where, according to equation (39), the high-order contributions have a vanishingly small size

$$|\rho_n(t)| \sim (J/\hbar\Gamma)^n |\rho_0(t)|, \quad t \gg J. \tag{41}$$

We are allowed to perform a self-consistent approximation which consists of, first, writing the evolution equations for each subspace $\rho_n(t)$, then imposing that all contributions $\rho_{n\geqslant 2} \simeq 0$ and finally integrating the remaining equations until we reach an effective model for the lowest order term.

5.2. Local projections

As sketched before, our study of the losses in the lattice begins by finding the eigenspaces of the unperturbed superoperator, $\mathcal{L}_{\text{int}}$. This task is greatly simplified by the fact that $\mathcal{L}_{\text{int}} = \sum_k \mathcal{L}_{\text{loc},k}$ is a sum of commuting local superoperators $\mathcal{L}_{\text{loc}}$. We can thus focus on diagonalizing one of these superoperators on a single lattice site.

We will now introduce some notation. Since we are interested in density matrices as elements of a Hilbert space on which the superoperators act, we will introduce a basis of vectors of this space. For a single site, we will define the basis of Fock states

$$|n, m) = \frac{1}{\sqrt{n!m!}} a^{\dagger n} |0\rangle\langle 0| a^m. \tag{42}$$

The scalar product between vectors is defined by introducing the adjoint basis $(n', m'|$ and the rule $(n', m'|n, m) = \delta_{nn'}\delta_{mm'}$. Equivalently, we can say that $(\rho_1|\rho_2) = \text{tr}(\rho_1^\dagger \rho_2)$. In this basis $\mathcal{L}_{\text{loc}}$ becomes a bidiagonal, non-symmetric operator

$$\mathcal{L}_{\text{loc}}|n, m) = -\frac{\mathrm{i}}{2\hbar} U_{\text{r}}(\xi_n - \xi_m)|n, m) - \frac{\Gamma}{4}(\xi_n + \xi_m)|n, m) + \frac{\Gamma}{2}\sqrt{\xi_n \xi_m}|n-2, m-2), \tag{43}$$

where $\xi_x = x(x-1)$. The kernel of this operator is given by states with 0 or one particle per site, so that we can write the space of non-decaying density matrices as in equation (12).

In addition to the right eigenvectors, $(\mathcal{L}_{\rm loc} - \lambda_n)|v_n) = 0$, we will also search the left eigenvectors, $(w_n|\mathcal{L}_{\rm loc} - \lambda_n) = 0$, which have the property $(w_n|v_m) = \delta_{nm}$. With these families of operators we will construct a set of pseudo-projector operators of the form

$$\mathcal{P}_n^{\rm loc} = |v_n)(w_n|. \tag{44}$$

We face one problem, though, which is that $\mathcal{L}_{\rm loc}$ acts on an infinite-dimensional space, with occupation numbers that can be arbitrarily large. We argue that for our purposes it suffices to truncate the Hilbert space to occupations $n, m \leqslant 2$. The reason is that our initial states will all belong to the space ρ_0 given above and, since we will neglect contributions from third and subsequent order couplings (i.e. $\rho_{2,3,\ldots} = 0$ in equation (40)), we will obtain at most a double occupation per site. The self-consistency of our approximation will be evident at the end.

Using the previous truncation, $\mathcal{L}_{\rm loc}$ becomes a 9×9 block-diagonal and banded matrix with projections onto eigenspaces

$$\mathcal{P}_0^{\rm loc} = |0,0)(2,2| + \sum_{b,b'=0,1} |b,b')(b,b'|, \tag{45a}$$

$$\mathcal{P}_{1a}^{\rm loc} = \sum_{b=0,1} |2,b)(2,b|, \tag{45b}$$

$$\mathcal{P}_{1b}^{\rm loc} = \sum_{b=0,1} |b,2)(b,2|, \tag{45c}$$

$$\mathcal{P}_2^{\rm loc} = |2,2)(2,2| - |0,0)(2,2| \tag{45d}$$

and corresponding eigenvalues

$$\lambda_0 = 0, \tag{46a}$$

$$\lambda_{1a} = -\frac{{\rm i}U}{\hbar} = -\frac{\Gamma}{2} - \frac{{\rm i}U_{\rm r}}{\hbar}, \tag{46b}$$

$$\lambda_{1b} = \lambda_{1a}^*, \tag{46c}$$

$$\lambda_2 = -\Gamma. \tag{46d}$$

$\mathcal{P}_{1a}^{\rm loc}$ and $\mathcal{P}_{1b}^{\rm loc}$ are connected to $\mathcal{P}_0^{\rm loc}$ by a single application of the hopping term, $\mathcal{V}$, and $\mathcal{P}_2^{\rm loc}$ by two applications of $\mathcal{V}$. Note also that $\mathcal{P}_0^{\rm loc}$ contains not only a projector onto single or zero occupancy, but also a term that destroys two particles at a site, emptying it. This will be essential later on.

5.3. Adiabatic elimination

As explained in section 3, we will consider that our states can be described by a density matrix with contributions coming from the eigenspace with the lowest decay rate, ρ_0, and the two eigenspaces connected to it, $\rho_{1a,1b}$. These contributions are, respectively, obtained by applying

the following pseudo-projectors onto $\rho(t)$:

$$\mathcal{P}_0 = \mathcal{P}_0^{\mathrm{loc}} \otimes \cdots \otimes \mathcal{P}_0^{\mathrm{loc}}, \tag{47a}$$

$$\mathcal{P}_{1a} = \sum_{m=0}^{L-1} (\mathcal{P}_0^{\mathrm{loc}})^{\otimes m} \otimes \mathcal{P}_{1a}^{\mathrm{loc}} \otimes (\mathcal{P}_0^{\mathrm{loc}})^{\otimes L-m-1}, \tag{47b}$$

$$\mathcal{P}_{1b} = \sum_{m=0}^{L-1} (\mathcal{P}_0^{\mathrm{loc}})^{\otimes m} \otimes \mathcal{P}_{1b}^{\mathrm{loc}} \otimes (\mathcal{P}_0^{\mathrm{loc}})^{\otimes L-m-1}. \tag{47c}$$

Note that the last two projectors are the sum of projectors onto different subspaces, each one containing a localized 'excitation' on a given lattice site. As such, the total projector includes all possible linear combinations of such states.

Connecting to the previous notation of projectors onto states with zero and one particles per site, it will be useful to realize that the zeroth-order projector can be written as follows:

$$\mathcal{P}_0 \rho = Q_0 \rho Q_0 + \frac{1}{2} \sum_k a_k^2 Q_1 \rho Q_1 a_k^{\dagger 2}. \tag{48}$$

Since we will neglect higher order couplings, we can use equations (10*a*) and (36) to write evolution equations for the density matrices in the form

$$\frac{\mathrm{d}\rho_0}{\mathrm{d}t} = \mathcal{V}_{00}\rho_0 + \sum_c \mathcal{V}_{0c}\rho_c, \tag{49a}$$

$$\frac{\mathrm{d}\rho_c}{\mathrm{d}t} = \lambda_c \rho_c + \mathcal{V}_{c0}\rho_0. \tag{49b}$$

We have abbreviated $\mathcal{V}_{ij} = \mathcal{P}_i \mathcal{V} \mathcal{P}_j$ and introduced the notation that the index c runs through $\{1a, 1b\}$. The terms ρ_c can be integrated out of the model using the fact that our states are initially prepared in the slow decaying manifold $\rho_c(0) = 0$. Formal integration of equation (49*b*) yields

$$\rho_c(t) = \mathrm{e}^{\lambda_c t} \int_0^t \mathrm{d}\tau \mathrm{e}^{-\lambda_c \tau} \mathcal{V}_{c0} \rho_0(\tau), \tag{50}$$

which after integration by parts becomes

$$\rho_c(t) = -\frac{1}{\lambda_c} \mathcal{V}_{c0} \left[\rho_0(t) - \mathrm{e}^{\lambda_c t} \rho_0(0)\right] + \frac{\mathrm{e}^{\lambda_c t}}{\lambda_c} \int_0^t \mathrm{d}\tau \mathrm{e}^{-\lambda_c \tau} \mathcal{V}_{c0} \frac{\mathrm{d}\rho_0}{\mathrm{d}t}(\tau). \tag{51}$$

We neglect the remaining integral, because it is of higher order in $J/\hbar\Gamma$ than the previous term, which is evident from the fact that $\mathrm{d}\rho_0/\mathrm{d}t \propto J$ in equation (49*a*). Insertion of $\rho_c(t)$ into equation (49*a*) yields

$$\frac{\mathrm{d}\rho_0}{\mathrm{d}t} = \left(\mathcal{V}_{00} - \sum_c \frac{1}{\lambda_c} \mathcal{V}_{0c} \mathcal{V}_{c0}\right) \rho_0(t) + \sum_c \frac{1}{\lambda_c} \mathrm{e}^{\lambda_c t} \mathcal{V}_{0c} \mathcal{V}_{c0} \rho_0(0). \tag{52}$$

The first line of this equation represents our effective model (16*a*) and will be discussed in the following section. The second line is a transient that decays at a rate $\propto \Gamma$. Therefore we obtained that the system converges to the slow-decaying eigenspace in a time $t \sim 1/\Gamma$, much shorter than the typical timescale $\hbar/J$ at which the effective model operates.

5.4. Hard-core bosons

Let us analyze the lowest order contribution to our effective model (52), given by $\mathcal{L}_1 = \mathcal{V}_{00}$. Using the expression in equation (48), we obtain

$$\mathcal{L}_1\rho_0 = \mathcal{P}_0\mathcal{V}\mathcal{P}_0\rho_0 = Q_0\frac{-\mathrm{i}}{\hbar}[H_J, Q_0\rho_0 Q_0]Q_0 = -\frac{\mathrm{i}}{\hbar}[Q_0 H_J Q_0, \rho_0]. \tag{53}$$

In other words, this Liouville operator is equivalent to a Hamiltonian in which we have projected out all states with double occupation. This is the hard-core bosons or Tonks–Girardeau gas model presented in section 3.2.

5.5. Second-order losses

We are now going to consider the second-order Liouvillian $\mathcal{L}_2$ from equation (16*a*)

$$\mathcal{L}_2 = \sum_{c\in\{1a,1b\}} \frac{-1}{\lambda_c}\mathcal{P}_0\mathcal{V}\mathcal{P}_c\mathcal{V}\mathcal{P}_0. \tag{54}$$

We can expand this expression

$$\mathcal{L}_2\rho_0 = \frac{-\mathrm{i}^2}{\lambda_{1a}\hbar^2}\mathcal{P}_0[H_J, Q_1[H_J, \rho_0]Q_0] + \frac{-\mathrm{i}^2}{\lambda_{1b}\hbar^2}\mathcal{P}_0[H_J, Q_0[H_J, \rho_0]Q_1]. \tag{55}$$

Using the property $\rho_0 = Q_0\rho_0 Q_0$, one realizes that the only relevant terms are $\mathcal{L}_2\rho_0 = \mathcal{P}_0\mathcal{A}\rho_0/\hbar^2$ with

$$\mathcal{A}\rho_0 = \frac{1}{\lambda_{1a}}\left(H_J Q_1 H_J Q_0\rho_0 - Q_1 H_J Q_0\rho_0 Q_0 H_J\right) + \frac{1}{\lambda_{1b}}\left(Q_0\rho_0 Q_0 H_J Q_1 H_J - H_J Q_0\rho_0 Q_0 H_J Q_1\right). \tag{56}$$

We now consider the final projection with $\mathcal{P}_0$. Following equation (48), this pseudo-projector contains two operations: the first one keeps terms proportional to $Q_0 H_J Q_1 H_J Q_0$, whereas the second one acts on the terms that create a doubly occupied site on each side of the density matrix that is $Q_1 H_J Q_0\rho_0 Q_0 H_J Q_1$. Introducing $T = Q_1 H_J Q_0/(-J)$,

$$\mathcal{L}_2\rho_0 = \frac{J^2}{\hbar^2}\left(\frac{1}{\lambda_{1a}}T^\dagger T\rho_0 + \frac{1}{\lambda_{1a}^*}\rho_0\, T^\dagger T\right) - \frac{2J^2}{\hbar^2}\left(\mathrm{Re}\frac{1}{\lambda_{1a}}\right)\frac{1}{2}\sum_k a_k^2 T\rho_0\, T^\dagger a_k^{\dagger 2}. \tag{57}$$

It is now time to rewrite everything in terms of hard-core boson operators. We notice the following equivalence:

$$T = Q_1\sum_{\langle k,l\rangle} a_k^\dagger a_l Q_0 = \sum_k a_k^{\dagger 2} C_k. \tag{58}$$

This arises from the fact that Q_1 projects onto a state with a single pair. Therefore, the tunneling term only contributes with processes that take two neighboring particles (C_k) and create a pair in one of the sites. Notice that C_k already enforces the projection Q_0. Using this notation we can simplify our expressions even further

$$a_k^2 T = 2C_k, \tag{59}$$

$$T^\dagger T = 2\sum_k C_k^\dagger C_k, \tag{60}$$

thus arriving at the final model

$$\mathcal{L}_2\rho_0 = \frac{2J^2}{\hbar^2}\sum_k\left(\frac{1}{\lambda_{1a}}C_k^\dagger C_k\rho_0 + \frac{1}{\lambda_{1a}^*}\rho_0 C_k^\dagger C_k\right) - \frac{2J^2}{\hbar^2}2\,\mathrm{Re}\frac{1}{\lambda_{1a}}\sum_k C_k\rho_0 C_k^\dagger, \quad (61)$$

which is studied in section 3.3.

6. Conclusion

We have shown analytically and confirmed numerically that strong, inelastic interactions can induce a Tonks–Girardeau gas dynamics for a cloud of molecules trapped in an optical lattice. The particles act like hard-core bosons, with dissipation playing the role of a strong repulsion. This effective model is completed with a reduced loss rate, $\gamma_{\mathrm{eff}} \propto J^2/\Gamma$, which is much slower than both the tunneling amplitude, $J/\hbar$, and the original loss rate, Γ.

Even with the small losses, the state of the system can be described at all times as an incoherent mixture of strongly correlated Tonks–Girardeau gases with different total particle number. In this respect, being based on the idea of using dissipation to create strong correlations, our paper connects to recent works which suggest using dissipation to engineer states and phase transitions [17, 18].

Our study can be generalized to consider other experimental features such as external fields. For instance, an additional harmonic trapping, if weak, will translate into the equivalent potential for the impenetrable bosons. This is the case in the experiments, where the focusing of the optical lattice beams causes a residual harmonic potential with a frequency of 70 Hz, too small to have significant effect during the molecule lifetime when the lattice is on. Note, on the other hand, that if the potential is such that it induces a site-to-site energy difference which is comparable to $\hbar\Gamma$, our approximations will break and it will be favorable for molecules to come together and anihilate, losing the hard-core nature. Finally, let us remark that the effect of temperature in current experiments is also negligible. Since the initial state is always a lattice gas of molecules with at most one particle per site, the initial temperature can only manifest in the form of imperfections in the lattice gas, that is holes. These holes will neither invalidate the previous mathematical models nor substantially alter the loss rates.

Acknowledgments

We acknowledge financial support of the German Excellence Initiative via the program Nanosystems Initiative Munich and of the Deutsche Forschungsgemeinschaft via SFB 631. JJG-R acknowledges financial support from the Ramon y Cajal Program of the MEC and from projects FIS2006-04885 and CAM-UCM/910758.

References

[1] Tonks L 1936 The complete equation of state of one, two and three-dimensional gases of hard elastic spheres *Phys. Rev.* **50** 955–63

[2] Girardeau M 1960 Relationship between systems of impenetrable bosons and fermions in one dimension *J. Math. Phys.* **1** 516–23

[3] Jordan P and Wigner E 1928 Über das paulische äquivalenzverbot *Z. Physik* **47** 631–51

[4] Lieb E H and Liniger W 1963 Exact analysis of an interacting Bose gas. I. The general solution and the ground state *Phys. Rev.* **130** 1605–16
[5] Paredes B, Widera A, Murg V, Mandel O, Fölling S, Cirac I, Shlyapnikov G V, Hänsch T W and Bloch I 2004 Tonks–Girardeau gas of ultracold atoms in an optical lattice *Nature* **429** 277–81
[6] Kinoshita T, Wenger T and Weiss D S 2004 Observation of a one-dimensional Tonks–Girardeau gas *Science* **305** 1125–8
[7] Kinoshita T, Wenger T and Weiss D S 2005 Local pair correlations in one-dimensional Bose gases *Phys. Rev. Lett.* **95** 190406
[8] Syassen N, Bauer D M, Lettner M, Volz T, Dietze D, Garcia-Ripoll J J, Cirac J I, Rempe G and Durr S 2008 Strong dissipation inhibits losses and induces correlations in cold molecular gases *Science* **320** 1329–31
[9] Verstraete F, Garcia-Ripoll J J and Cirac J I 2004 Matrix product density operators: simulation of finite-temperature and dissipative systems *Phys. Rev. Lett.* **93** 207204
[10] Dürr S, García-Ripoll J J, Syassen N, Bauer D M, Lettner M, Cirac J I and Rempe G 2008 Lieb–Liniger model of a dissipation-induced Tonks–Girardeau gas arXiv:0809.3696
[11] Calderia A O and Leggett A J 1981 Influence of dissipation on quantum tunneling in macroscopic systems *Phys. Rev. Lett.* **46** 211–4
[12] Marquardt F and Golubev D S 2005 Many-fermion generalization of the Calderia–Leggett model *Phys. Rev.* A **72** 022113
[13] Jaksch D, Bruder C, Cirac J I, Gardiner C W and Zoller P 1998 Cold bosonic atoms in optical lattices *Phys. Rev. Lett.* **81** 3108–11
[14] Cazalilla M A 2003 One-dimensional optical lattices and impenetrable bosons *Phys. Rev.* A **67** 053606
[15] Volz T, Syassen N, Bauer D M, Hansis E, Dürr S and Rempe G 2006 Preparation of a quantum state with one molecule at each site of an optical lattice *Nat. Phys.* **2** 692–5
[16] Kato T 1995 *Perturbation Theory for Linear Operators* (Berlin: Springer) chapter II
[17] Verstraete F, Wolf M M and Cirac J I 2008 Quantum computation, quantum state engineering, and quantum phase transitions driven by dissipation arXiv:0803.1447
[18] Diehl S, Micheli A, Kantian A, Kraus B, Büchler H P and Zoller P 2008 Quantum states and phases in driven open quantum systems with cold atoms arXiv:0803.1482